43

ИНСТИТУТ ЯДЕРНОЙ ФИЗИКИ СО АН СССР

G.P. Berman, F.M. Izrailev, O.F. Vlasova

QUASI-ENERGY FUNCTIONS AND QUASI-ENERGY SPECTRUM OF TWO INTERACTING NONLINEAR RESONANCES IN THE REGION OF CLASSICAL CHAOS

PREPRINT 86-181

НОВОСИБИРСК

Quasi-Energy Functions and Quasi-Energy Spectrum of Two Interacting Nonlinear Resonances in the Region of Classical Chaos

G.P.Berman, F.M. Izrailev, O.F. Vlasova**

Institute of Nuclear Physics
630090, Novosibirsk, USSR

ABSTRACT

The structure of quasi-energy functions and spectrum of quasi-energies of two interacting nonlinear resonances are investigated. Main attention is devoted to the properties of a quantum system in the case when stochastic motion appears in the classical limit due to overlapping of nonlinear resonances. The role of quantum effects under the conditions of classical chaos is discussed.

* L.V. Kirensky Institute of Physics, 660036, Krasnoyarsk, USSR.

INTRODUCTION

Recently considerable attention is devoted to the study of interaction of highly-excited atoms and molecules (Rydberg states) with external monochromatic radiation (see, e. g. [1, 2]). Since we discuss the quasi-classical region of occupation of system levels where the constant of anharmonicity is small, sufficiently strong excitation involves a large number of levels in dynamics. Thereby a particular form of excitation analogous to classical stochastic diffusion can appear. Mechanism of such diffusion in classical mechanics is studied quite well and is based on the phenomenon of overlapping of nonlinear resonances [3—5]. Dynamics of a quantum system at the interaction of a large number of nonlinear resonances has been considered both for simple models (see, e . g. [4, 6, 7]) and ones similar to real systems [8—10]. In these examples stochasticity appears in a large region of phase space and may lead to global instability. At the same time there are systems in which stochasticity is limited by relatively small region of phase space. The typical example is interaction of two nonlinear resonances which describes, for instance, motion of electron in the field of two plasma waves [11].

In the quantum case dynamics of interaction of two nonlinear resonances was studied in Refs [12, 13], where it has been shown particularly that at overlapping of nonlinear resonances and sufficiently large value of quasi-classical parameter behavior of the quantum system at finite times is analogous to stochastic behavior of the corresponding classical system. With time increasing, however, quantum effects occur resulting in suppressing dynamical chaos [4, 6, 12, 13].

Note that while studying behavior of nonautonomous quantum system two approaches may be used: study of system dynamics (diffusion, time correlations etc.) and analysis of spectral characteristics (spectrum of quasi-energies and structure of quasi-energy eigenfunctions [14, 15]). When the first approach is comparatively well developed, properties of quasi-energy spectrum and, in particular, structure of eigenfunctions for quantum systems which are stochastic in the classical limit are less studied. However, in real experiments on exciting atoms and molecules in periodic fields spectral approach in some cases is more natural. From this point of view theoretical study of quasi-energy spectrum characteristics of quantum systems with chaotic behaviour seems to us very important.

In the present paper the results of investigation of spectral properties in quantum systems of two interacting nonlinear resonances are given. Description of the model and methods of numerical investigation of quasi-energy spectrum and quasi-energy eigenfunctions are given in Section 2. The case of critical values of perturbation parameter corresponding in the classical limit to the contact of primary resonances is considered in Section 3. Also the structure of eigenfunctions depending on perturbation parameter is analized. Statistical properties of quasi-energy eigenfunctions in the region of quantum chaos are investigated in Section 4. Statistics of spacings between neighbouring levels of quasi-energies in dependence on selection of eigenfunctions according to parameter of their localization is studied in Section 5. In conclusion the main results of the work are briefly summerized.

2. DESCRIPTION OF THE MODEL

As a model convenient for study of interaction of two nonlinear resonances we choose a quantum rotator in the field of two waves [12, 13]:

$$\hat{H}=-\gamma\hbar^2\frac{\partial^2}{\partial\theta^2}+V_1\cos(\theta+\nu t)+V_2\cos(\theta-\nu t). \qquad (2.1)$$

Hamiltonian (2.1) arises, for example, by analysis of dipole interaction of the external field (containing two frequencies resonant to different levels of unperturbed spectrum) with nonlinear quantum system in the region of quasi-classical occupation. In such an example γ is the parameter of nonlinearity of unperturbed spectrum, ν is the difference of the resonant frequencies of the external field; $V_{1,2}$ are the amplitudes of the external fields [12, 13].

In the classical limit Hamiltonian (2.1) takes the form:

$$H=\gamma I^2+V_1\cos(\theta+\nu t)+V_2\cos(\theta-\nu t) \qquad (2.2)$$

where I is the classical action of the system. Hamiltonian (2.2) describes interaction of two nonlinear resonanses which position is determined by the equations:

$$\omega(I_1)=2\gamma I_1=-\nu; \quad \omega(I_2)=2\gamma I_2=\nu \qquad (2.3)$$

where $I_{1,2}$ are the resonant values of action. If $V_1=0$ (or $V_2=0$) put into (2.2) the system is reduced to an isolated nonlinear resonance that is exactly integrated and characterized by the following parameters: ΔI is the width of action and Ω is the frequency of phase oscillations in the vicinity of resonance

$$(\Delta I)_{1,2}=2\sqrt{\frac{2V_{1,2}}{\gamma}}; \quad \Omega_{1,2}=\sqrt{2\gamma V_{1,2}}. \qquad (2.4)$$

For the description of interaction of two nonlinear resonances the parameter of their overlapping is introduced [3]:

$$K=\frac{(\Delta I)_1/2+(\Delta I)_2/2}{I_2-I_1}=\frac{2\sqrt{2\gamma V}}{\nu} \qquad (2.5)$$

where $V_1=V_2=V$. It is easy to show that the parameter K (2.5) is the only dimensionless parameter determining completely dynamics of classical system.

At $K\ll 1$ each of nonlinear resonances is well isolated, and a particle cannot pass from the region of one resonance into the region of another. In this case motion in large part of phase space is regular (for the exception of narrow regions in the vicinity of separatrices of resonances). Qualitatively new effect comes at $K\gtrsim 1$, when the interaction of resonances becomes essential. In the latter case chaotic motion becomes global in the sense that stochastic trajectory does not occupied only the vicinity of one resonance but can go from one resonance to another.

Analysis of the system dynamics (2.2) and the structure of phase space is given in [3, 16, 17]. For illustration we present here the structure of phase plane of the system (2.2) at different values of parameter K (see Fig. 1). As it may be seen for $K \approx 1.33$ (Fig. 1,*b*) inside the stochastic region there are large enough islands where stochastic trajectory does not penetrate. Analysis shows that in these islands motion has stable and regular character. With increase of parameter K up to $K \approx 4.5$ the distruction of large islands occurs. Fig. 1,*c* shows a typical example of phase plane at such values of parameter K when measure of stable islands inside stochastic region is small.

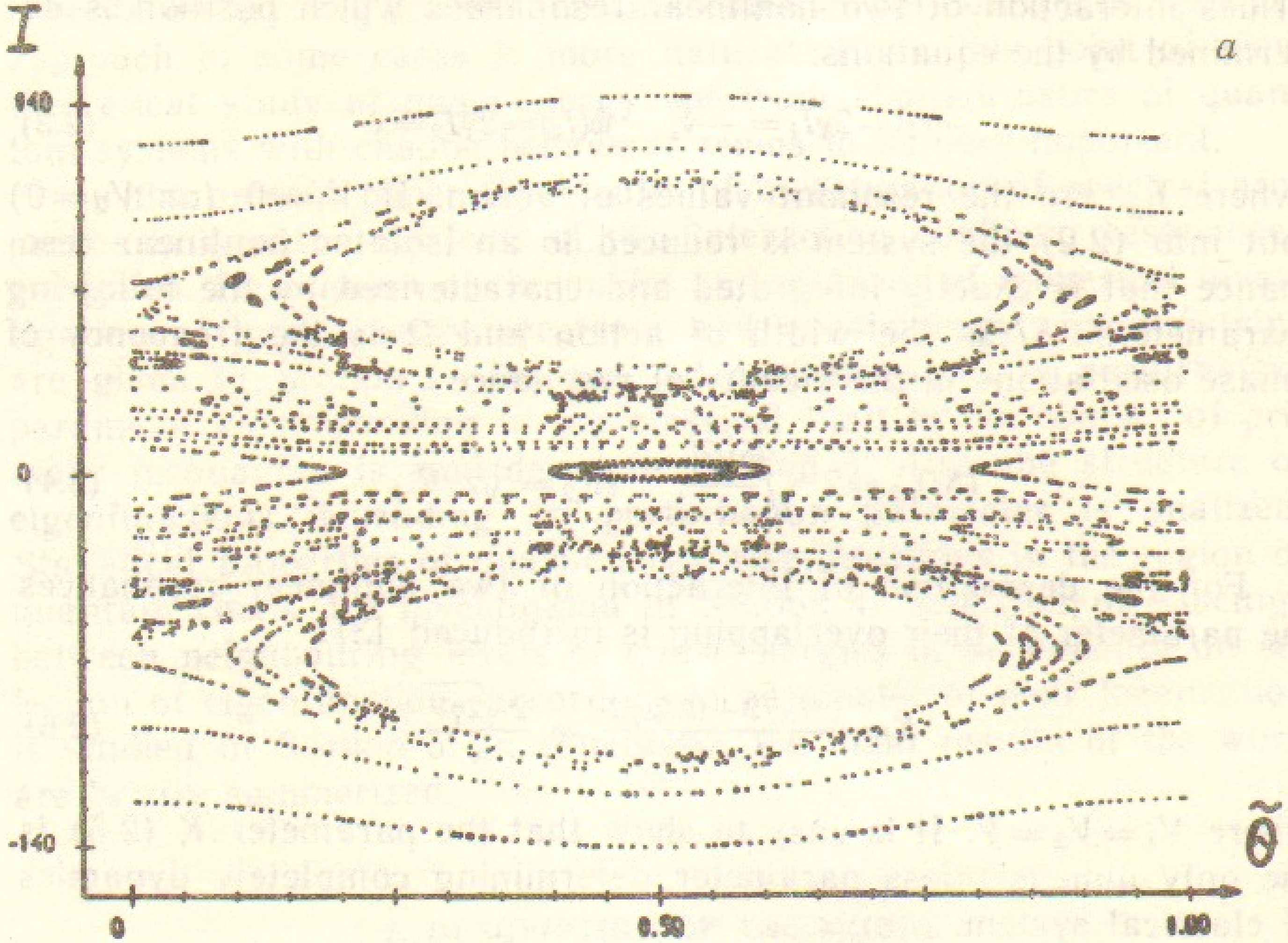

Fig. 1. Structure of phase plane of the classical system (2.2) for $V=20$; $\gamma=2.5\cdot10^{-2}$. Points in the Fig. 1,*a*,*b*,*c* correspond to values I, $\tilde{\theta}=\theta/2\pi$ at time moments $t_m=2\pi m/\nu$ (through the period of external field T). Fig. 1,*a* depicts 46 trajectories with different initial values I_0, θ_0 during 100 periods ($T_m \leqslant 100\ T$), Fig. 1,*b*,*c* shows one stochastic trajectory ($t_m \leqslant 2000$). Parameters of the system (2.2) are: *a*) $K \approx 0.57$, $\nu=3.5$; *b*) $K \approx 1.33$, $\nu=1.5$; *c*) $K \approx 4.44$, $\nu=0.45$.

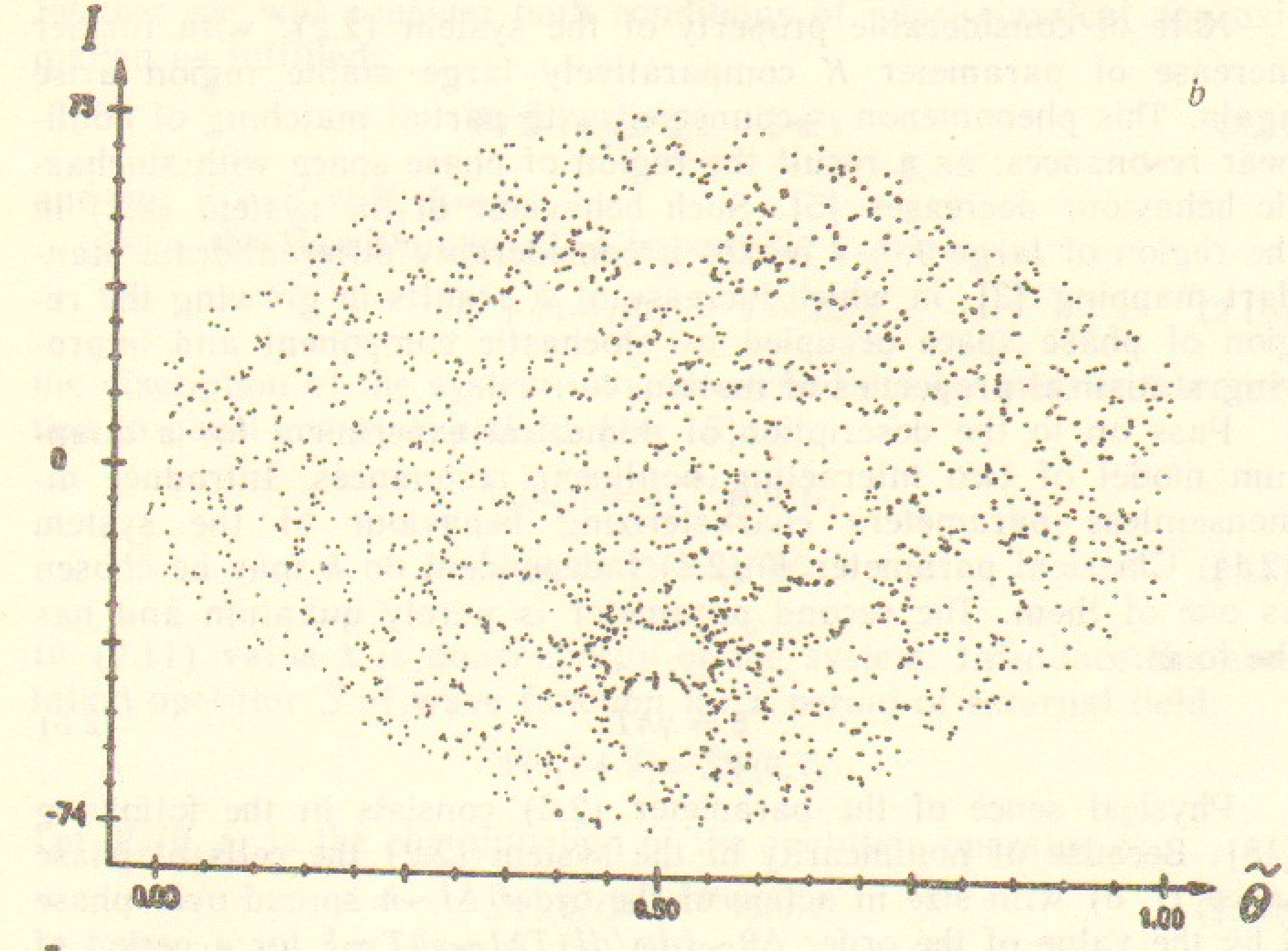

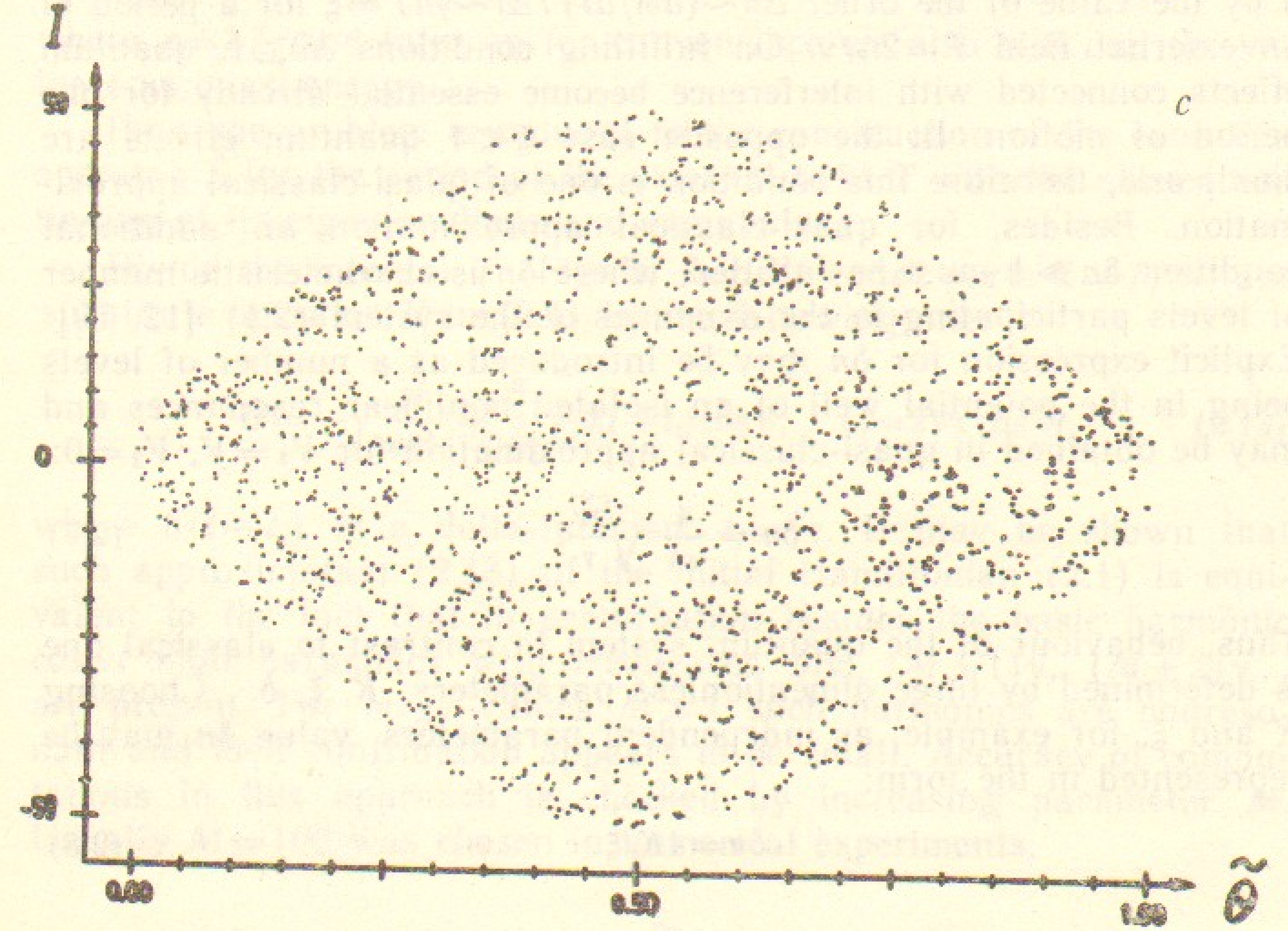

Note of considerable property of the system (2.2): with further increase of parameter K comparatively large stable region arise again. This phenomenon is connected with partial matching of nonlinear resonances; as a result the region of phase space with stochastic behaviour decreases [5]. Such behaviour of the system (2.2) in the region of large $K \gg 1$ makes it considerably different from standart mapping [3], in which increase of K results in growing the region of phase space occupied by stochastic component and improving statistical properties of motion.

Pass on to the description of numerical experiment for a quantum model of two interacting nonlinear resonances. Introduce dimensionless parameters characterizing behaviour of the system (2.1). Classical parameter K (2.5) independent on $\hbar$ may be chosen as one of them. The second parameter is purely quantum and has the form:

$$\xi = \gamma \hbar T. \qquad (2.6)$$

Physical sence of the parameter (2.6) consists in the following [18]. Because of nonlinearity of the system (2.2) the cells of phase space (I, θ) with size in action of the order $\Delta I \sim \hbar$ spread over phase θ by the value of the order $\Delta\theta \sim (d\omega/dI)\, T \Delta I \sim \gamma \hbar T = \xi$ for a period of an external field $T = 2\pi/\nu$. On fulfilling conditions $\Delta\theta \gtrsim 1$, quantum effects connected with interference become essential already for one period of motion. In the opposite case $\xi \ll 1$ quantum effects are small and, therefore this condition is one of quasi-classical approximation. Besides, for quasi-classical approximation an additional condition $\delta n \gg 1$ must be fulfilled, where δn is characteristic number of levels participating in the dynamics of the system (2.1) [12, 19]. Explicit expression for δn may be introduced as a number of levels being in the potential well of an isolated nonlinear resonances and may be obtained in quasi-classical approximation for $V_1 = V$, $V_2 = 0$:

$$\delta n = \frac{4}{\pi \hbar} \sqrt{\frac{2V}{\gamma}}. \qquad (2.7)$$

Thus, behaviour of the quantum system in contrast to classical one is determined by three dimentionless parameters: K, ξ, δ. . Choosing K and ξ, for example, as independent parameters, value δn may be represented in the form:

$$\delta n = 4K/\xi. \qquad (2.8)$$

Further we will consider both conditions of quasi-classical approximation as fulfilled:

$$\delta n \gg 1\ (K \gg \xi); \quad \xi \ll 1 \qquad (2.9)$$

and put $V_1 = V_2 = V$; $\hbar = 1$.

Since the Hamiltonian (2.1) is periodic in time:

$$\hat{H}(t+T) = \hat{H}(t); \quad T = 2\pi/\nu \qquad (2.10)$$

the discription of the system may be carried out by means of transition to quasi-energy functions [14, 15]:

$$\Psi_\lambda(\theta, t) = e^{-i\lambda t} \varphi_\lambda(\theta, t),$$

$$\varphi_\lambda(\theta, t+T) = \varphi_\lambda(\theta, t). \qquad (2.11)$$

In (2.11) value λ is quasi-energy of the system. Introduce the evolution operator $\hat{S}$ of wave function for a period of external field:

$$\Psi(\theta, t+T) = \hat{S}\Psi(\theta, t)$$

Let $\Psi_\varepsilon(\theta, t)$ is the eigenfunction of the evolution operator $\hat{S}$:

$$\hat{S}\Psi_\varepsilon(\theta, t) = e^{-i\varepsilon} \Psi_\varepsilon(\theta, t) \qquad (2.12)$$

where $\varepsilon = \lambda T$, and later on for convenience we also will call the value ε as quasi-energy.

Thus, the problem is reduced to the construction of the evolution operator $\hat{S}$ for the period of the external field T with the subsequent finding of its eigenfunctions and eigenvalues.

Divide the interval T (Fig. 2) into M equal parts $\tau = T/M$, and substitute operator $\hat{H}$ in (2.1) by the following one:

$$\hat{H} = -\gamma \frac{\partial^2}{\partial \theta^2} + \sum_{j=1}^{M} v_j \delta(t - t_j) \cos\theta; \quad v_j = 2V\tau \cos \nu t_j \qquad (2.13)$$

where $\delta(t - t_j)$ is a delta-function, $t_j = j\tau$. It may be shown that such approximation (2.13) of the initial Hamiltonian (2.1) is equivalent to the fact that in perturbation besides the basic harmonic $\cos \nu t$ high harmonics with frequences $M\nu$, $(M \pm 1)\nu$, $(M \pm 2)\nu$ ... are present. For large values $M \gg 1$ such harmonics are nonresonant and their contribution appears to be small. Accuracy of computations in this approach is checked by increasing parameter M. Usually $M = 100$ was chosen in numerical experiments.

As a result the evolution operator $\hat{S}=\hat{S}_{t=0}$ may be represented in the following form:

$$\hat{S}=\hat{S}_1\hat{S}_2 \ldots \hat{S}_j \ldots \hat{S}_{M-1}\hat{S}_M \qquad (2.14)$$

where

$$\hat{S}_j=\exp\left(-i\frac{\tau\gamma}{2}\frac{\partial^2}{\partial\theta^2}\right)\exp(-iv_j\cos\theta)\exp\left(-i\frac{\tau\gamma}{2}\frac{\partial^2}{\partial\theta^2}\right). \qquad (2.15)$$

Since the initial Hamiltonian is invariant in respect to the change of the sign θ, the quasi-energy eigenfunctions may be classified by pa-

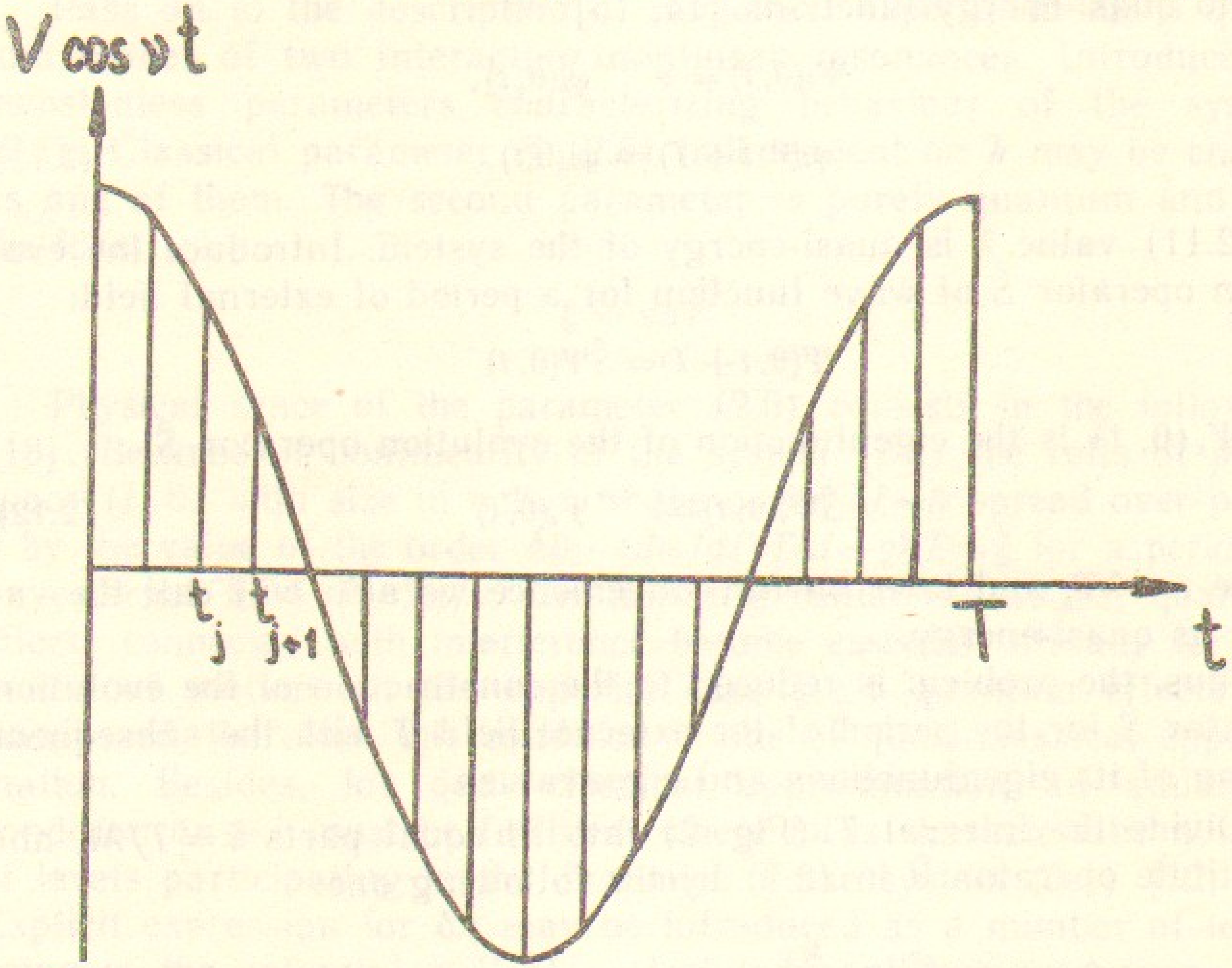

Fig. 2. Approximation (2.13) of the potential of the initial system (2.1).

rity. Further to simplify computations we will consider only antisymmetric functions $\Psi_\varepsilon(-\theta, t)=-\Psi_\varepsilon(\theta, t)$. Choose as a basis antisymmetric functions of unperturbed operator:

$$|n\rangle=\frac{1}{\sqrt{\pi}}\sin n\theta; \quad (n=1, 2, \ldots). \qquad (2.16)$$

In the representation (2.16) matrix elements of the operator $\hat{S}_j$ have the form:

$$S_{nm}(j)\equiv\langle n|\hat{S}_j|m\rangle=\exp\left(i\frac{\tau\gamma n^2}{2}\right)B_{nm}\exp\left(i\frac{\tau\gamma m^2}{2}\right). \qquad (2.17)$$

where

$$B_{nm}=\frac{1}{2N+1}\sum_{l=1}^{2N+1}\left[\cos(n-m)\frac{2\pi l}{2N+1}-\cos(n+m)\frac{2\pi l}{2N+1}\right]\times$$

$$\times\exp\left(-iv_j\cos\frac{2\pi l}{2N+1}\right), (n, m=1, \ldots, N). \qquad (2.18)$$

In (2.18) parameter N is equal to the total number of states (2.16) in numerical experiment. The criterium of the choice of the value N was a weak change of the eigenfunctions and eigenvalues in the investigated region of phase space of interacting resonances with N increasing (usually $N=89$; 151 was chosen).

Note that matrices $S_{nm}(j)$ (2.17) **are** symmetric and unitary. As a result the finite matrix S_{nm} resulting from multiplication of matrices (2.17) has the same properties of symmetry. The symmetry of the unitary matrix S_{nm} testifies to conservation of invariance in the model with the finite number of levels in respect to time reversal (in accordance with the properties of the initial system (2.1)). Thus, numerical analysis is reduced to determination of quasi-energy spectrum and quasi-energy eigenfunctions of symmetric matrix S_{nm}:

$$S_{nm}=\sum_{m_1,\ldots,m_M}S_{nm_1}(1)\,S_{m_1m_2}(2)\ldots S_{m_Mm}(M). \qquad (2.19)$$

3. THE STRUCTURE OF QUASI-ENERGY FUNCTIONS IN THE CRITICAL REGION ($K\sim1$)

First of all dwell on the properties of eigenfunctions of an isolated nonlinear resonance that may be obtained from (2.1) assuming, for example, that $V_1=V$; $V_2=0$. In this case the Hamiltonian of an isolated resonance takes the form [12, 13]:

$$\hat{H}=-\gamma\hbar^2\frac{\partial^2}{\partial\vartheta^2}+V\cos\vartheta \qquad (3.1)$$

where $\vartheta=\theta+\nu t$, and transition to a new wave function $\varphi(\vartheta, t)$ is made:

$$\varphi(\vartheta, t) = \exp[i(l_1\vartheta - \gamma\hbar l_1 t)]\ \Psi(\vartheta, t) \tag{3.2}$$

in (3.2) l denotes the number of resonant level satisfying to the condition (see left equality in (2.3)):

$$2\gamma\hbar l_1 = -\nu\,. \tag{3.3}$$

The problem of determining eigenfunctions of the Hamiltonian (3.1) is reduced to the solution of Mathieu equation:

$$\gamma\hbar^2 \frac{d^2\varphi_\varepsilon(\vartheta)}{d\vartheta^2} + (\varepsilon - V\cos\vartheta)\,\varphi_\varepsilon(\vartheta) = 0; \qquad \varphi_\varepsilon(\vartheta + 2\pi) = \varphi_\varepsilon(\vartheta)\,. \tag{3.4}$$

Solution of the equation (3.4) are periodic Mathieu functions Fourier series of which have in general case sufficiently complicated structure. Therefore determination of the form of these functions was carried out numerically. Fig. 3 shows quasi-energy eigenfunctions $\varphi_\varepsilon(\vartheta)$ of coupled states in unperturbed basis $(1/\sqrt{2\pi})\exp(in\vartheta)$. It is clear that the number of eigenstates in the potential well $V\cos\vartheta$ agrees well with quasi-classical estimate (2.7): $\delta n \approx 36$. As numerical data show for $\delta n \gg 1$ the structure of eigenfunctions near separatrix (edges of the well) becomes considerably more complicated. It is natural to expect with perturbation such eigenfunctions are subjected to stronger change with possible appearance of irregularity in their structure (see Sec. 4). Above the separatrix $\varepsilon_l > V$ quasi-energy functions sufficiently quickly approximate to asymptotic expressions $\sin(l\vartheta)$ and $\cos(l\vartheta)$; in Fig. 3 it would correspond to two peaks (Fourier-amplitudes) $A_{\pm|l|}$.

For quantitative characteristic of the structure of eigenfunctions corresponding to energy levels for $\varepsilon_l > V$ it is convenient to introduce the following values [20]:

$$l = 2\left[\sum_{n=-\infty}^{\infty} (n - \bar{n})^2 |A_n|^2\right]^{1/2}; \qquad \bar{n} = \sum_{n=-\infty}^{\infty} n|A_n|^2. \tag{3.5}$$

In (3.5) A_n are coefficients of expansion of the eigenfunction $\varphi_\varepsilon(\vartheta)$ into functions $(1/\sqrt{2\pi})\exp(in\vartheta)$. The value $\bar{n}$ determines «center of gravity» of the function $\varphi_\varepsilon(\vartheta)$; l is its mean-square width $\left(\sum_n |A_n|^2 = 1\right)$. Fig. 4 shows the dependence of l on the number of the eigenstate n_ε. As it is seen from Fig. 4 the effective width l of

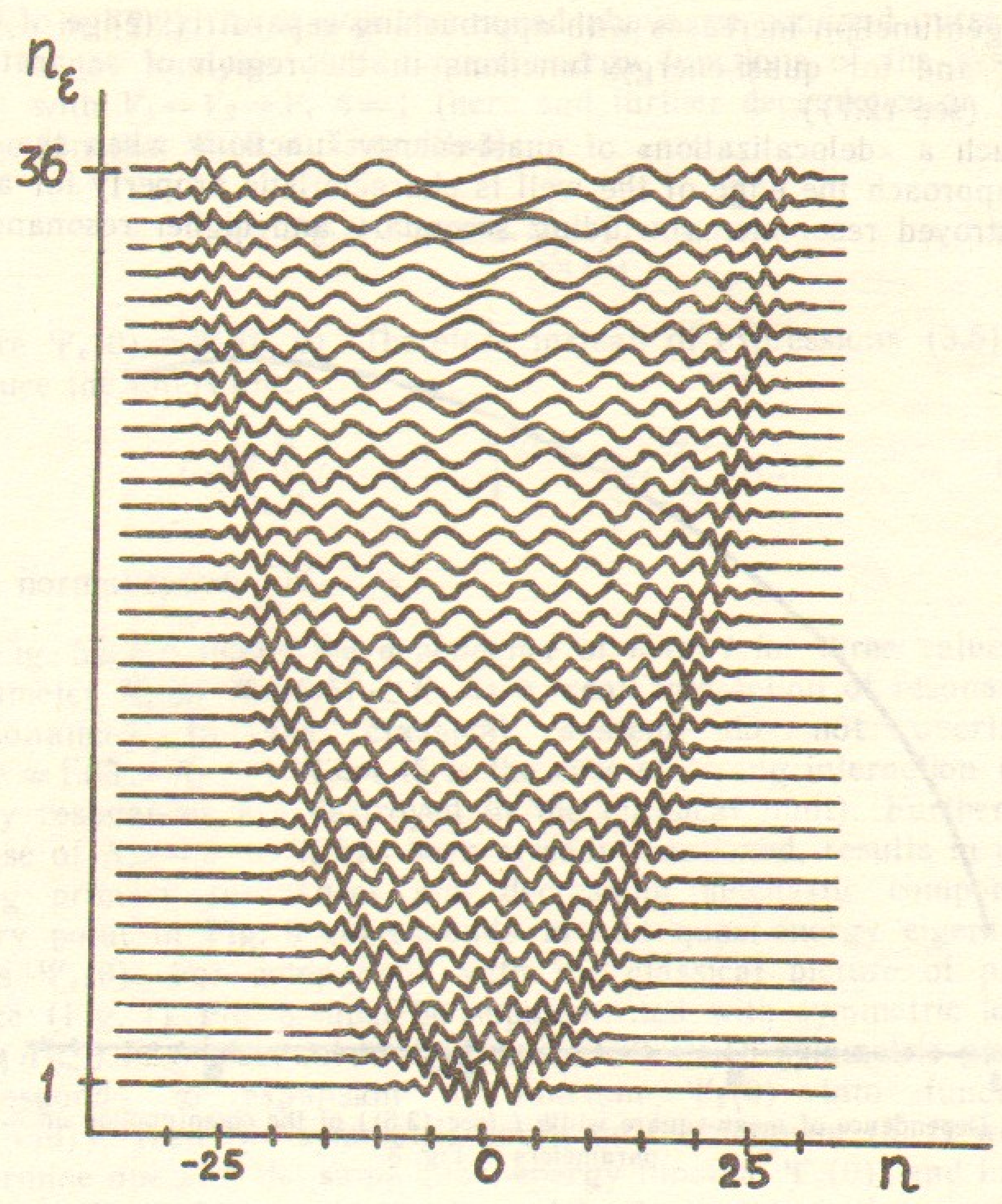

Fig. 3. Quasi-energy functions of an isolated resonance in the basis of unperturbed $(V_1 = V_2 = 0)$ states. Fourier-amplitudes C_n of all eigenfunctions of the coupled states $(\varepsilon < V)$ of the system (3.4) with parameters $V = 0.2$; $\gamma = 5 \cdot 10^{-4}$, $\hbar = 1$ are shown. Value n_ε corresponds to the number of the eigenfunction n_ε are reading from the bottom of the potential well.

the eigenfunction increases with approaching separatrix (edge of the well), and for quasi-energy functions in the region of separatrix $l_s \sim \delta n$ (see (2.7)).

Such a «delocalization» of quasi-energy functions when the levels approach the edge of the well is characteristic property for any undestroyed resonance (including secondary and higher resonances

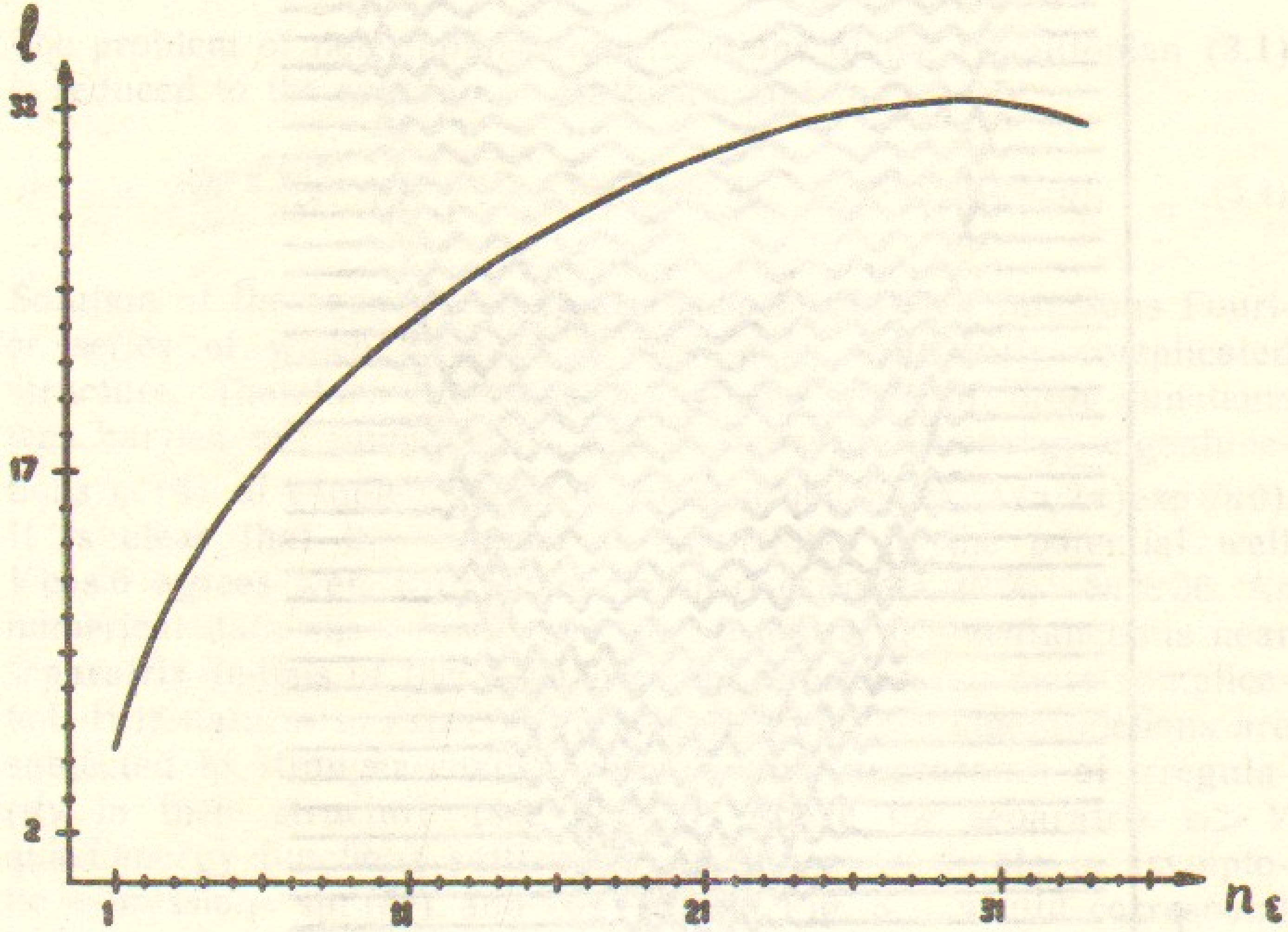

Fig. 4. Dependence of mean-square width l (see (3.5)) of the eigenfunction on n_ε for parameters in Fig. 3.

of the system (2.1)). Therefore an approximate estimation takes place: $l_s^{(m)} \sim \delta n(V_m)$ where V_m is the depth of the potential well of m-th resonance. In the classical case the structure of the phase space is self-similar when one goes from large to small scales [16—17], therefore certain properties of renormalization for the value $l_s^{(m)}$ [21] also take place.

Now pass on to the description of the structure of quasi-energy functions in the system (2.1) of two interacting resonances in the transition region $K \gtrsim K_{cr}$ where according to [16] the value K_{cr} is given by the estimate $K_{cr} \approx 0.71$ and corresponds to the destruction of the last invariant curve of rotation lying between classical reso-

nances in (2.2). As it was mentioned above we confined ourselves only to the analysis of odd quasi-energy functions of the system (2.1) with $V_1 = V_2 = V$, $\hbar = 1$ (here and further dependence on time in the function $\Psi_\varepsilon(\theta, t)$ is omitted):

$$\Psi_\varepsilon(-\theta) = -\Psi_\varepsilon(\theta) = \frac{1}{\sqrt{\pi}} \sum_{n=1}^{\infty} C_n \sin n\theta \qquad (3.6)$$

where $\Psi_\varepsilon(\theta) \equiv \Psi_\varepsilon(\theta, 0)$. Therefore instead of expressions (3.5) introduce the following:

$$l = 2\left[\sum_{n=1}^{\infty} (n - \bar{n})^2 |C_n|\right]^{1/2}; \quad \bar{n} = \sum_{n=1}^{\infty} n |C_n|^2 \qquad (3.7)$$

with normalization $\sum_n |C_n|^2 = 1$.

Fig. 5,*a*,*b*,*c* shows the dependence of $\bar{n}$ on l for three values of parameter K; *a*) $K \approx 0.57 < K_{cr}$ is a weak interaction of resonances (resonances in the classical system do not overlap); *b*) $K \approx 1.33 > K_{cr}$; *c*) $K \approx 4.45$ is the case of strong interaction (primary resonances are destroyed in the classical limit). Further increase of $K > 4.5$, as it has been already mentioned, results in matching primary resonances and decreasing stochastic component. Every point in Fig. 5 corresponds to odd quasi-energy eigenfunctions $\Psi_\varepsilon(\theta)$. For comparison with the classical picture of phase space (Fig. 1) Fig. 5 must be supplemented with symmetric lower part $\bar{n} < 0$ in respect to straight line $\bar{n} = 0$ (such symmetric picture corresponds to expansion of function $\Psi_\varepsilon(\theta)$ into functions $\exp(in\theta)$). Then two symmetric points on the diagram $(\bar{n}, l)$ would determine one and the same quasi-energy function $\Psi_\varepsilon(\theta)$, and in the classical limit they would correspond to the motion in two parts of phase space with $I > 0$ and $I < 0$.

From Fig. 5,*a* it is seen that points corresponding to different $\Psi_\varepsilon(\theta)$ lie mainly on three branches; further we will call this picture «a beak». The upper part of the beak corresponds to functions $\Psi_\varepsilon(\theta)$ lying above the edges of potential wells of primary resonances (classical trajectories of «untrapped» particles correspond to them). Eigenfunctions of the levels being inside the potential wells of the primary resonances correspond to the points on the horizontal branch of the beak. The lower branch of the beak in Fig. 5,*a* corresponds to functions $\Psi_\varepsilon(\theta)$ situated on the diagram $(\bar{n}, l)$ between

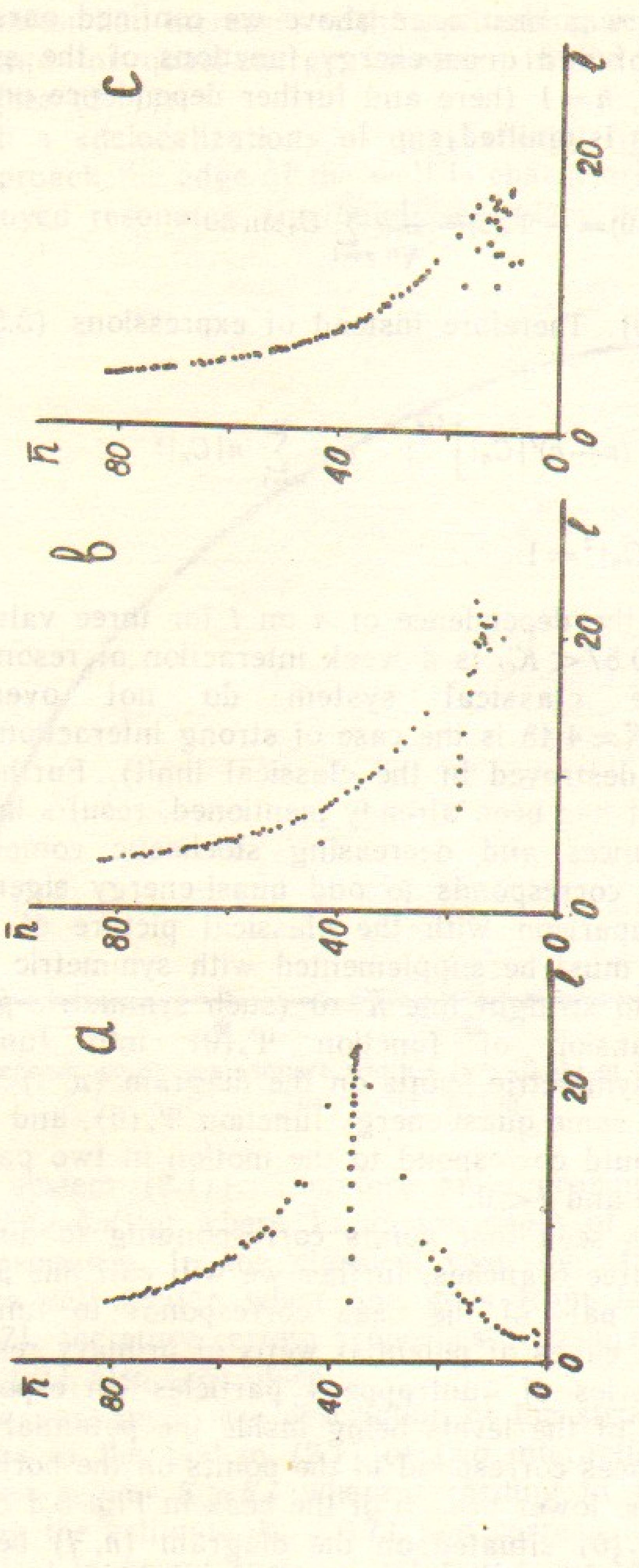

Fig. 5. «Centre of gravity» dependence $\bar{n}$ of the eigenfunction on its mean-square width l for the system (2.1) with parameters $V_1=V_2=10$, $\gamma=5\cdot10^{-2}$, $\delta n\approx25.5$. Fig. 5,*a* — classical resonances do not overlap, $K\approx0.57$, $\nu\approx3.5$; Fig. 5,*b* — weak overlapping of resonances, $K\approx1.33$, $\nu=1.5$; Fig. 5,*c* — strong overlapping of resonances, $K\approx4.4$, $\nu=0.45$.

primary resonances and half-integer resonance (vicinity of $\bar{n}\approx0$, in Fig. 1,*a* — vicinity $l\approx0$). Note two circumstances: 1) the points on the horizontal branch with small l correspond to eigenfunctions lying near the bottom of the potential wells of primary resonances, and such functions are, in this sense, well localized; 2) the lower branch of the beak in Fig. 5 includes some points of the upper branch of the beak of half-integer resonance (small «splash» in the neighbourhood $\bar{n}\approx0$ on the lower part of Fig. 5,*a*). The most delocalized eigenfunctions corresponding to the vicinity of separatrices of primary resonances are situated at the top of the big beak.

Of great importance is the fact that each undestroyed resonance with number m corresponds to its m-th beak having main peculiarities of Fig. 5,*a* but on a smaller scale, since the depth of its potential well decreases with m increase. With regard of the chosen in Fig. 5,*a* parameters, estimates show that the number of odd eigenfunctions connected with half-integer resonance is approximately 5. It means, according to (2.9), that quasi-classical condition is not well satisfied. Correspondingly, the beak of this resonance not completely destroyed.

In the other limiting case of strong interaction (Fig. 5) the main and half-integer resonances are destroyed and correspondingly the horizontal branch of the large beak and the whole lower branch are destroyed as well. Only the upper branch of the beak corresponding to high-lying states remained undestroyed. We should note the irregular character of eigenfunctions belonging to the top of the large destroyed beak in Fig. 5,*c*. They are not only delocalized (large $l\gg1$) but, as it is seen from Fig. 5,*c*, points corresponding to them are situated on the diagram $(\bar{n}, l)$ irregularly. It means that in the structure of these states itself there must be a certain portion of irregular component. This problem will be discussed later.

Now dwell on characteristic pecularities of destruction of the lower branch in Fig. 5,*a*. This problem presents a particular interest since destruction of this branch is connected with the destruction of half-integer resonance lying in the region $\bar{n}\approx0$. In other words, we are interested in the character of destruction of eigenfunctions near the separatrix of half-integer resonance that in the classical limit corresponds to the destruction of the last invariant curve between primary resonances. Fig. 6,*a* shows the destruction of the lower branch with increase of the overlap parameter K (the upper branch in Fig. 6 is not given). As it is clear from Fig. 6 this destruction takes place because of the destruction of half-integer resonance and besides in irregular manner (low points in Fig. 6,*b*,*c*). The primary resonances thereby do not destroy (points on the horizontal branch remain). With destructing eigenfunctions of the lower branch rearrange—delocalize (l increases) and are displaced on the diagram ($\bar{n}$, l) into the region of the top of the beak of primary resonances where they are also irregularly disposed (the latter is connected with the destruction of separatrices of primary resonances). Such irregular character of delocalization of quasi-energy functions is the quantum manifestation of classical chaos. More detailed peculiarities of the character of destruction of the lower branch require additional investigations including increase of matrices demension used in the procedure of numerical diagonalization of the evolution operator $\hat{S}$.

4. QUASI-ENERGY FUNCTIONS IN THE REGION OF MAXIMUM CHAOS

Now pass on to the problem of statistical properties of quasi-energy functions in the region of maximum chaos when primary resonances are completely destroyed. For this purpose consider quasi-energy functions belonging to the top of destroyed beak. Figs 7,*a*,*b* show Fourier-expansion of two typical quasi-energy functions with different regions of their localization. It is naturally to assume that eigenfunctions of the type shown in Fig. 7,*a* being in the region of stochasticity formed by overlapping of two basic resonances of classical system will have the most statistical properties. Points on the diagram ($\bar{n}$, l) corresponding to these eigenfunctions arrange in irregular manner and refer to the lowermost, distroyed part of the beak (see Fig. 5,*c*). It may be expected that such states in the restricted region $1 < n \leqslant n_{cr}$ possess not only the property of ergodicity [22] but also the distribution similar to Gaussian one [23, 24] (see also [25]).

Statistical analysis of eigenfunctions was carried out by the following manner. According to numerical data value $n_{cr} = 48$ is chosen in such a way that the localization length of the chosen eigenfunctions would be more than n_{cr}. Then the region along n is divided into four equal parts and for each of them histogram of distributions of the value $x_n = \mathrm{Re}\, C_n$ in respect to the average value $\langle x_n \rangle \approx 0$ is constructed. To improve statistics histograms for diffe-

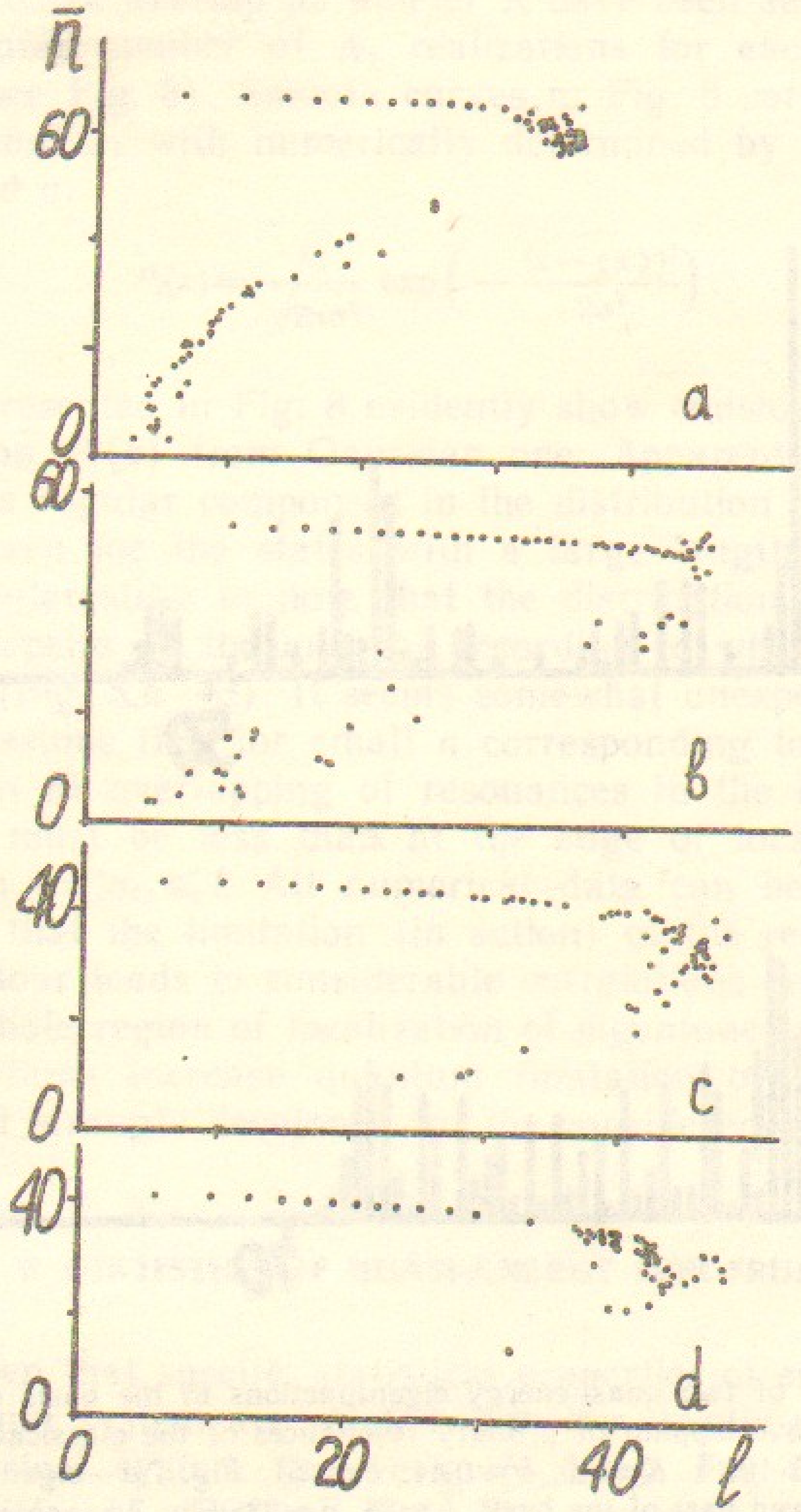

Fig. 6. Destruction of the lower branch of «the beak» with increase of the overlap parameter K: $\delta n \approx 51$, $V = 20$, $\gamma = 2.5 \cdot 10^{-2}$; Fig. 6,*a* — $K = 0.625$, $\nu = 3.2$; Fig. 6,*b* — $K = 0.8$, $\nu = 2.5$; Fig. 6,*c* — $K = 1.0$, $\nu = 2$; Fig. 6,*d* — $K = 1.176$, $\nu = 1.7$.

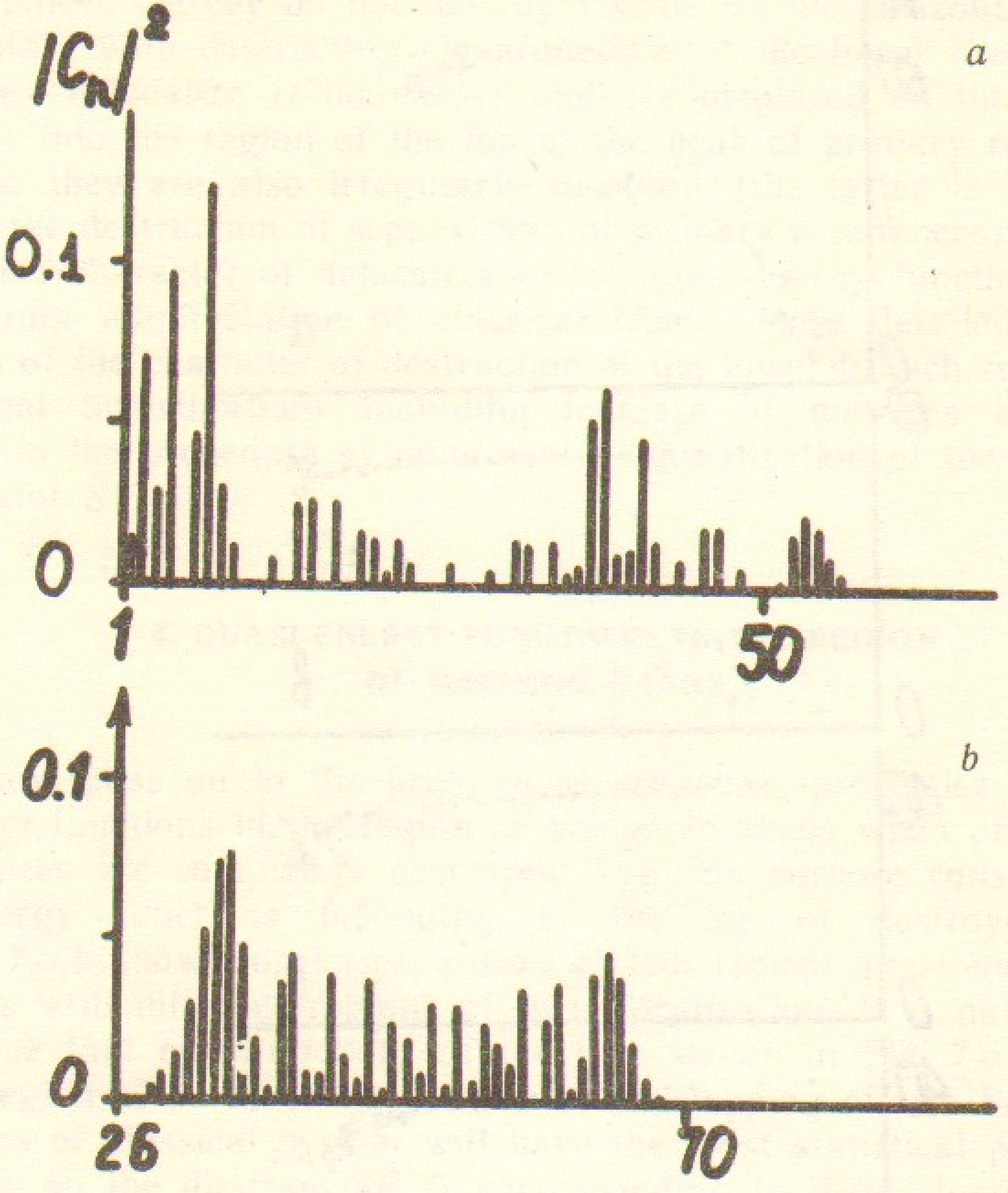

Fig. 7. An example of two quasi-energy eigenfunctions in the basis of unperturbed states with strong overlapping of primary resonances of the classical system (2.2): $V_1=V_2=20$; $\gamma=2.5\cdot10^{-2}$; $K\approx4.5$, $\nu\approx0.44$, $\delta n\approx51$. Fig. 7,*a*—eigenfunctions from the region of destroyed part of the beak, $L\approx36$, $\bar{n}\approx23$; Fig. 7,*b*—eigenfunction from the transition region of the upper branch of the beak, $l\approx24$, $\bar{n}\approx46$.

rent values of the overlap parameter K have been summed up. As a result the total number of N_1 realizations for each histogram is $N_1=1956$ (see Fig. 8). Smooth curves in Fig. 8 correspond to Gaussian distribution with numerically determined by histograms values $\langle x\rangle$ and σ:

$$P_f(x)=\frac{N_1}{\sqrt{2\pi\sigma^2}}\exp\left(-\frac{(x-\langle x\rangle)^2}{2\sigma^2}\right). \tag{4.1}$$

Data represented in Fig. 8 evidently show considerable deviation of distribution $P_f(x)$ from Gaussian one. Apparently it means the presence of a regular component in the distribution of Fourier-amplitudes C_n even for the states with a large length of localization $l\gg1$. It is interesting to note that the distribution $P_f(x)$ does not practically depend on the interval according to which the summing up is made (Fig. 8,*a*—*d*). It seems somewhat unexpected since it is natural to assume that for small n corresponding to the most destroyed region at overlapping of resonances in the classical model correlations must be less than at the edge of localization of the eigenfunction $n\lesssim n_{cr}\lesssim l$. All numerical data can be interpreted in such a way that the limitation (in action) of the region with stochastic behaviour leads to considerable correlations between amplitudes in the whole region of localization of eigenfunctions. As a result such correlations increase quantum limitation of classical chaos (which is not strongly developed for the considered model).

5. STATISTICS OF QUASI-ENERGY SPECTRUM

It is known that specific statistical properties of energy spectrum of the quantum system are related with the chaotic motion of autonomous classical system (see, e. g. [4, 26]). For the quantitative description different statistical tests [27] are used, particularly, distribution $P(s)$ of distances between neighbouring levels of energy in the spectrum of the system. In statistical description of complicated quantum systems such as heavy nuclei and atoms the dependence $P(s)$ is one of the most important characteristics in the Wigner—Dyson theory [28—29]. In the simplest case $P(s)$-dependence has the form:

$$P(s)=As^{\beta}e^{-Bs^2} \tag{5.1}$$

where s is the distance between the nearest levels, A, B are normalization constants, β is the parameter determining the degree of repulsion of neighbouring levels. As it follows from Ref. [29] the value of the parameter $\beta=1;\ 2;\ 4$ is connected with the symmetry of the initial system.

In Refs [30—31] it has been shown that Wigner—Dyson distribution takes also place for nonautomonous systems (with perturbation periodically dependent on time) which are stochastic in the classical limit (see also [32]). In this case dependence $P(s)$ describes distribution of distances between neighbouring levels of quasi-energy reduced to interval $2\pi/T$, where T is a period of perturbation.

For our system (2.1) distribution $P(s)$ for all quasi-energies ε_l in the case of maximum chaos $K\approx4.4$ has the form represented in Fig. 9,*a*. Here, as well as earlier, to improve statistics the ensemble consisting of several systems (2.1) with different values of stochasticity parameter K has been used. For comparison Poisson distribution is represented in Fig. 9,*a*:

$$P(s)=\frac{N_l}{\Delta}e^{-s/\Delta} \qquad (5.2)$$

which can sufficiently well describe distribution $P(s)$ for the systems which are integrable in the classical limit (see [33], as well as discussion in [34]). From Fig 9,*a* it is clear that numerical data for $P(s)$ are much closer to the dependence (5.2) than to Wigner—Dyson distributions (5.1). Note that owing to invariance in respect to time reversal both for the initial system (2.1) and for the model (2.13—2.19) only value $\beta=1$ should be considered [31]. In spite of not bad qualitative agreement of dependence $P(s)$ in Fig. 9,*a* with Poisson distribution slight deviation in the region of small $s\ll\Delta$ is noticeable. Proximity of distribution $P(s)$ to Poisson one is not suprising since statistical treatment was carried out with all eigenvalues, the most part of which corresponds to strongly localized states. The latter include also the states corresponding to stable classical motion out of resonance (rotation). Therefore it is natural to consider statistics of eigenvalues of those quasi-energy states that have large width $l\gg1$ and to a certain extent are irregular.

Fig. 9,*b* shows distribution $P(s)$ for those eigenvalues which correspond to the most delocalized eigenfunctions of quasi-energies

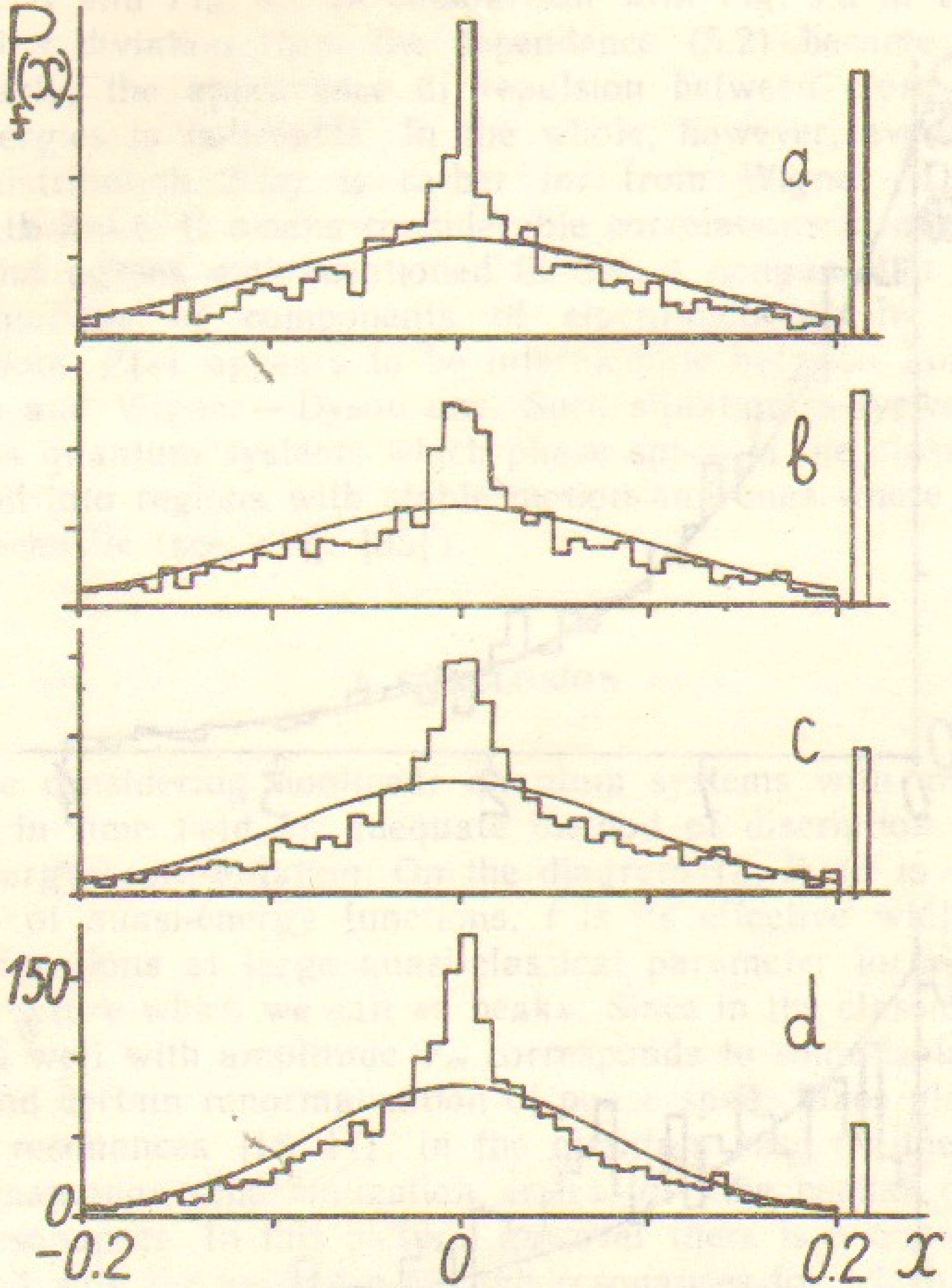

Fig. 8. Histogram of distribution of the value $x_n=\mathrm{Re}\,C_n$ for eigenfunctions with a big length of localization $l\gg1$ at strong overlapping of resonances $V=20$, $\gamma=2.5\cdot10^{-2}$, $\delta n\approx51$, $N_l=1956$, $n_{cr}=48$. The overlap parameter K changed withing the limits $4.5\leqslant K\leqslant5.1$. Smooth curve—Gaussian distribution (4.1). Data for different sections of unperturbed states are given: *a*) $1\leqslant n\leqslant12$; *b*) $13\leqslant n\leqslant24$; *c*) $25\leqslant n\leqslant36$; *d*) $37\leqslant n\leqslant48$. A separate peak shows the number of values with $|x|>0.2$.

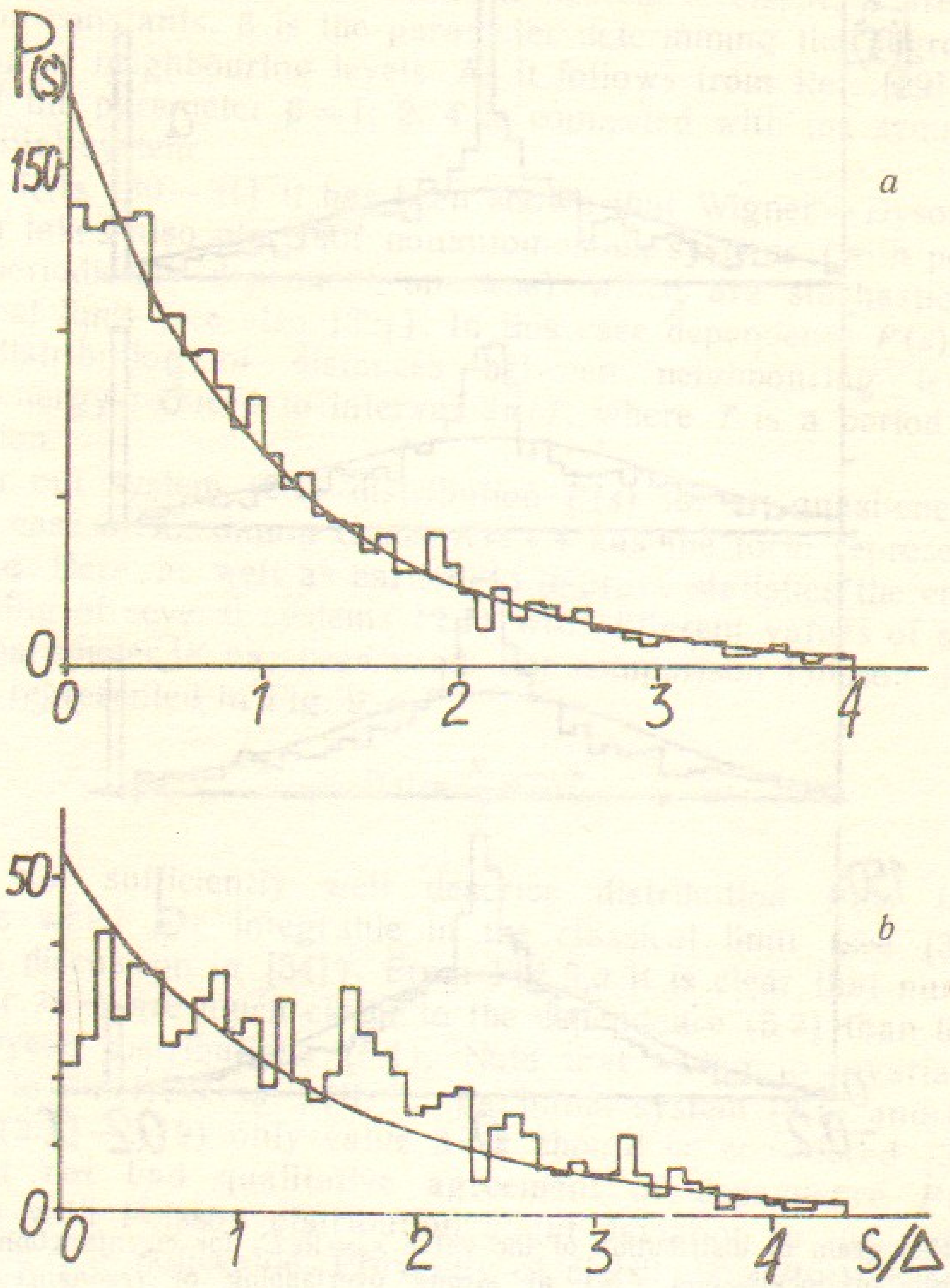

Fig. 9. Distribution $P(s)$ of distances between neighbouring values of quasi-energy for $V=20$, $\gamma=2.5\cdot10^{-2}$, $\delta n\approx51$. Value Δ corresponds to mean distance between levels: $\Delta=2\pi/N$. Smooth curve — Poisson distribution (5.2). Fig. 9,*a* — distribution $P(s)$ for all eigenvalues: $N_1=2047$, $4.31\leqslant K\leqslant4.52$; $0.44\leqslant\nu\leqslant0.46$. Fig. 9,*b* — distribution $P(s)$ for the most delocalized and irregular states, $N_1=778$; $31\leqslant K\leqslant4.46$; $0.45\leqslant\nu\leqslant0.46$.

(see Sec. 4 and Fig. 8). In comparison with Fig. 9,*a* in the region of small *s* diviation from the dependence (5.2) became stronger. Particularly, the appearance of repulsion between close levels of quasi-energies is noticeable. In the whole, however, even for such states distribution $P(s)$ is rather far from Wigner — Dyson one (5.1) with $\beta=1$. It means considerable correlations in quasi-energy states and agrees with mentioned in Sec. 4 nongaussian character of fluctuations of components of eigenfunctions. In this case distributions $P(s)$ appears to be intermediate between Poisson distribution and Wigner — Dyson one. Such situation is typical for autonomous quantum systems which phase space in the classical limit is divided into regions with stable motion and ones where the motion is stochastic (see, e. g. [35]).

6. CONCLUSION

While considering nonlinear quantum systems with an external periodic in time field an adequate method of discription is one of quasi-energy representation. On the diagram $(\bar{n}, l)$ ($\bar{n}$ is «center of gravity» of quasi-energy functions, l is its effective width) quasi-energy functions at large quasi-classical parameter form characteristic structure which we call «a beak». Since in the classical limit a potential well with amplitude V_m corresponds to some isolated resonance and certain renormalization of phase space takes place owing to high resonances [16, 17], in the quantum case on the diagram $(\bar{n}, l)$ analogous renormalization arises for «the beaks» of undestroyed resonances. In this picture, however there is a quantum limit connected with the existance of high resonances for which the number of trapped levels is small [21].

It is known that in the classical system the distruction of resonances is accompanied by the appearance of regions with chaotic component. In the first turn these regions appear in the vicinity of separatrices of interacting resonances. In the quantum case an analog of classical stochasticity in terms of quasi-energy eigenfunctions is their reconstruction with appearance of irregularity on the diagram $(\bar{n}, l)$ and with their delocalization. The latter means considerable reconstruction of quasi-energy function owing to the increase of the number of harmonics of unperturbed spectrum containing in it (see Fig. 7).

Analysis of distributions of delocalized quasi-energy functions corresponding to destroyed resonances and distribution of distances between the nearest levels of quasi-energies shows the presence of considerable correlations. The latter are related both with the restriction of chaotic area in the phase space of the classical system and with the quantum effects leading to the limitation of classical chaos.

We are greatly indebted to B.V. Chirikov for the constant attention to this work and useful comments and to A.R. Kolovsky and D.L. Shepelyansky for discussions.

REFERENCES

1. Rydberg States of Atoms and Molecules. Ed. P. Stebbings and F. Danning, Cambridge University Press, 1983.
2. *Delone N.B., Krainov V.P., Shepelyansky D.L.* Usp. Fiz. Nauk, 1983, v.140, p.355.
3. *Chirikov B.V.* Phys. Rep., 1979, v.52, p.263.
4. *Zaslavsky G.M.* Stochasticity of Dynamic Systems. M: Nauka, 1985.
5. *Lichtenberg A.J., Lieberman M.A.* Regular and Stochastic Motion (Springer Verlag, New York, 1983).
6. *Chirikov B.V., Izrailev F.M. Shepelyansky D.L.* Sov. Sci. Reviews, 1981, v.2C, p.209.
7. *Berman G.P., Kolovsky A.R.* Physica, 1983, v.D8, p.117.
8. *Casati G., Chirikov B.V., Guarneri I., Shepelyansky D.L.* Phys. Rev. Lett., 1986, v.56, p.2437.
9. *Izrailev F.M.* Physica, 1981, v.D2, p.243.
10. *Berman G.P., Zaslavsky G.M., Kolovsky A.R.* JETP, 1985, v.88, p.1551.
11. *Doveil F.* Phys. Rev. Lett., 1981, v.46, p.532.
12. *Berman G.P., Zaslavsky G.M., Kolovsky A.R.* JETP, 1984, v.81, p.506.
13. *Berman G.P., Zaslavsky G.M., Kolovsky A.R.* Phys, Lett., 1982, v.A87, p.152.
14. *Zeldovich Ya.B.* JETP, 1966, v.51, p.1492.
15. *Ritus V.I.* JETP, 1966, v.51, p.1544.
16. *Escande D.F., Doveil F.* J. Stat. Phys., 1981, v.26, p.257.
17. *Escande D.F.* Phys. Rep., 1985, v.121, p.167.
18. *Berman G.P., Zaslavsky G.M.* Physica 1982, v.A111, p.17.
19. *Shuryak E.V.* JETP, 1976, v.71, p.2039.
20. *Toda M.* Phys. Lett., 1985, v.A110, p.235.
21. *Berman G.P., Vlasova O.F., Izrailev F.M, Kolovsky A.R.* Preprint N 402, Krasnoyarsk, 1986.
22. *Shnirelmann A.I.* Usp. Math. Nauk, 1974, v.29, p.181.
23. *Porter C.E., Tomas R.G.* In: Statistical Theories of Spectra: Fluctuations.—Acad. Press N.Y and London, 1965, p.167.
24. *Berry M.V.* J. Phys. A: Math. Gen., 1977, v.10, p.2083.
25. *Chirikov B.V.* Phys. Lett., 1985, v.A108, p.68.
26. *Bohigas O., Giannoni M. J.* Lecture Notes in Physics, 1984, v.209, p.1.

27. *Brody T.A., Flores J., French J.B., Mello P.A., Pandey A., Wong S.S.M.* Rev. of Mod. Phys., 1981, v.53, p.385.
28. *Wigner E.P.* In: Statistical Theories of Spectra: Fluctuations.—Acad. Press N.Y. and London, 1965, p.88, 145, 176, 226.
29. *Dyson F.J.* J. Math. Phys., 1962, v.3, p.140, 157, 166 (trans.: F. Dyson. Statistical Theory of Energy Levels of Complicated Systems. M.: In. Lit., 1963).
30. *Izrailev F.M.* Preprint 84-63, Novosibirsk, 1984.
31. *Izrailev F.M.* Phys. Rev. Lett., 1986, v.56, p.541.
32. *Jose J.V., Cordery R.* Phys. Rev. Lett., 1986, v.56, p.290.
33. *Berry M.V., Tabor M.* Proc. Roy. Soc. of London, A.: Math. Phys. Sc., 1977, v.356, p.375.
34. *Casati G., Chirikov B.V., Guarneri I.* Phys. Rev. Lett., 1985, v.54, p.1350.
35. *Seligman T.N., Verbaarshot J.J.M., Zirnbauer M.R.* Phys. Rev. Lett., 1984, v.53, p.215; J. Phys. A.: Math. Gen., 1985, v.18, p.2751.

G.P.Berman, F.M. Izrailev, O.F. Vlasova

Quasi-Energy Functions and Quasi-Energy Spectrum of Two Interacting Nonlinear Resonances in the Region of Classical Chaos

Г.П. Берман, Ф.М. Израйлев, О.Ф. Власова

Квазиэнергетические функции и спектр квазиэнергий двух взаимодействующих нелинейных резонансов в области классического хаоса

Ответственный за выпуск С.Г.Попов

Работа поступила 15 декабря 1986 г.
Подписано в печать 30.12. 1986 г. МН 11919
Формат бумаги 60×90 1/16 Объем 2,0 печ.л., 1,6 уч.-изд.л.
Тираж 250 экз. Бесплатно. Заказ № 18

*Набрано в автоматизированной системе на базе фотонаборного автомата ФА1000 и ЭВМ «Электроника» и отпечатано на ротапринте Института ядерной физики СО АН СССР,
Новосибирск, 630090, пр. академика Лаврентьева, 11.*